Crosswell tomography imaging of the permeability structure within a sandstone oil field.

Tokuo Yamamoto[(1)], and Junichi Sakakibara[(2)]

[(1)] *University of Miami and Yamamoto Engineering Corporation,* [(2)] *Kawasaki Steel Corporation.*

ABSTRACT

Imaging the permeability structure of the earth is a challenge of geophysics. The first case of the permeability structure image within a limestone aquifer was obtained from a set of acoustic crosswell tomography data through an analytical inversion based on a new poroelastic theory called the super-k model (Yamamoto, 1998). In this paper we present the second example image of permeability structure within a sandstone oil reservoir. High quality data of acoustic crosswell tomography were obtained by a newly built system of the pseudo-random binary sequence (PRBS) based crosswell tomography (U.S. Patent No. 5,406,530). The velocity and attenuation images measured at a 500 Hz PRBS were inverted analytically based on a squirt flow theory. The acoustically measured permeability images agree with the permeability information gathered through down hole logs and cores.

KEY WORDS: permeability, crosswell geophysics, acoustics, images, sandstone reservoir.

INTRODUCTION

Imaging the permeability structure of the earth acoustically has been and is a challenge of geophysics. It requires a high quality acoustic image measurement method, physically consistent predictive models of acoustic wave propagation through earth, and accurate and stable inversion techniques.

Because the physics of acoustic wave propagation through earth is very complicated, there is no single theory that can accurately model the physics for all earth materials. It has been shown by Yamamoto et al (1994) that the Biot (1956) theory predicts the acoustic wave propagation through saturated, non-cemented sediments at frequencies between 1 and 10 kHz. For sandstone, the squirt flow theory by Mavko and Nur (1975) have been shown to predict adequately for the wave propagation at crosswell frequencies and ultrasonic frequencies. Dvorkin and Nur (1993) combined the Biot theory and the squirt flow theory. Yamamoto (1998) has developed a new poroelastic theory for very permeable limestone and accurately inverted the crosswell acoustic tomography data for permeability. Some other theories may be needed for fractured volcanic rock formations. All these theories require the rock properties as given input. Empirical equations for bulk modulus and shear modulus of skeletal frame are usually used for this purpose.

From the point of view of inversion calculations, the simpler the model the better. From this point of view, the BISQ (Biot and Squirt flow) model by Dvorkin and Nur (1993) is too complicated to find the correct permeability inverse from measured acoustic data. It has been shown that the analytical super-k model of limestone (Yamamoto, 1998) is accurate and stable for permeability inversion for limestone. Similarly, it will be shown that the squirt flow model is suitable for inversion of acoustic data for the permeability image within sandstone oil reservoirs.

SQUIRT FLOW THEORY

An analytical inverse theory for the permeability within sandstone formation is built using the squirt flow theory. Readers are refered to Mavko and Nur (1975); Dvorkin and Nur (1993); and Yamamoto (1998) for the physics and mathematics behind the theory. The acoustic wave slowness **s** is given by the squirt flow theory as

$$\mathbf{s}^2 = \frac{\rho}{M + \mathbf{F}_{sq}\,\alpha^2 / \phi} \qquad (1)$$

where ρ is the bulk density of the sediment, M is the uniaxial modulus of the frame, α is a Biot elastic coefficient, and ϕ is porosity. In this paper, vectors and complex variables are expressed by bold letters. $\mathbf{F}_{sq}$ is the squirt flow modulus of pore fluid given by,

$$\mathbf{F}_{sq} = F\left[1 - \frac{2 J_1(\lambda R)}{\lambda R J_0(\lambda R)}\right] \qquad (2)$$

where F is the Biot elastic modulus of pore fluid stiffness, R is the squirt flow length, and J_0 and J_1 are the Bessel

functions of the order zero and one. The squirt flow wave number λ is given through the following nondimensionsal equation;

$$(\lambda R)^2 = i\frac{\omega\mu\phi R^2}{Fk} = i\,\Omega \qquad (3)$$

where ω is the angular frequency $2\pi f$, f is the frequency, μ is the viscosity of pore fluid, and k is the permeability. The phase velocity V_P and the intrinsic attenuation Q^{-1} of the super-k medium are given as:

$$V_P = 1/\,\mathrm{Real}(\mathbf{s}), \quad \text{and}$$
$$Q^{-1} = 2\,\mathrm{Imag}(\mathbf{s})\,/\,\mathrm{Real}(\mathbf{s}) \qquad (4)$$

As mentioned earlier, the elastic moduli of the skeletal frame have to be estimated from the measured sound speed V_P. The empirical relation of Han et al. (1986) is used to estimate the shear modulus and bulk modulus of the skeletal frame. The values of clay content c were assumed for sandstone and shale. The Biot coefficient F and α are then calculated using the Biot (1956) equations.

PERMEABILITY INVERSE

The permeability inverse is obtained through equations 1 through 4. First, the elastic moduli and porosity estimates are obtained from the measured velocity V_P through the Han et al. (1986) sandstone formula. Then the permeability is inverted from the measured attenuation Q^{-1}. It should be noted that the attenuation and the velocity dispersion are only the function of a dimension less, real positive value parameter; Ω. Therefore, if one find the unique values of Ω that satisfy the equations 4, one can find the permeability through equation 3 as,

$$k = \frac{\omega\mu\phi R^2}{F\,\Omega} \qquad (5)$$

If the permeability is known from other measurements, the viscosity of the pore fluid is inverted as,

$$\mu = \frac{Fk\,\Omega}{\omega\phi R^2} \qquad (6)$$

This analytical inversion is simple and very stable as will be shown in the following.

CROSSWELL ACOUSTIC TOMOGRAPHY

The crosswell tomography experiment using the new system YEC2111 was conducted in May and June of 1998 using wells MD15 and Q1 at an oil field of TOL (TRINCAN OIL LTD), Trinidad. The resistivity logs and gamma-ray logs of the two wells are reproduced in Figures 1 a and b. The two oil wells are separated by a horizontal distance of 125 m. The cross-section between the two wells and between the depths 350 m and 800 m was imaged at 500 Hz PRBS of 4095 cycles, with a source and receiver depth interval of 6 m. This produces a total of 60,000 source-receiver rays. The number of stacking or averages varied from 100 to 400, making total compression of up to 160,000 pulses. Due to the powerful source out put of the new source ITC 6145 (180 dB at 500 Hz, 198 dB at 1000 Hz, and 210 dB between 1500 and 5000 Hz), the test experiment of the new system YEC2111 went very smoothly and finished in 2 days once the experiment became ready.

A 95 % of the 60,000 rays measured during the crosswell experiment is used in inversion analysis because of the extremely good quality of the wave data. A typical source gather after correlation is plotted in Figure 2. Clear first arrival waves are easily recognizable from the source gather. Therefore, the inverted velocity and attenuation images are of high quality and give a high confidence in the inverted images. The least squares SVD (Singular Value Decomposition) inversion codes for velocity and attenuation by Bregman et al. (1989) were used in the calculations. The pair of velocity and attenuation images are given in Figure 3 a and b. The examination of images clearly show that the imaged section can be roughly divided into four subsections: sand layer 350 to 450 m, shale layer 450 to 530 m, sand layer 530 to 650 m, and shale layer 650 to 800 m. These rough subdivisions of the section agree with the electric and gamma ray logs of the two wells. Actual geology of the section is much more complicated than these simplified divisions as will be seen in the permeability images.

POROSITY IMAGES

The proposed permeability inversions requires the values of porosity, shear modulus and bulk modulus of skeletal frame, viscosity of pore fluid, and squirt flow length. The porosity, shear modulus and bulk modulus are estimated from the velocity image Figure 3 a using the Han et al. (1986) empirical formula. The extraction procedure is presented in Yamamoto et al. (1995). The sandstone porosity and the shale porosity images extracted by this procedure are shown in Figure 4 a and b. The clay content of the sandstone is assumed at 25 % in the calculation and 95 % for the shale. These porosity and

elastic modulus values are used in the permeability inversions.

MEASURED PERMEABILITY IMAGES

The permeability images for the sand layers (350-450 m, and 530-650 m) and the shale layers (450-530 m, and 650-800 m) are inverted through the analytical inverse procedure and shown in Figure 5 a and b. In the inversion calculations, a measured viscosity, 4.0 mPa s, of the oil from the two wells, and constant squirt flow lengths 500 μm for the sandstone and 20 μm for the shale are assumed. According to the analytical permeability inversion, the top sandstone layer at 350-450 m has permeability between 180 and 200 md and the bottom sandstone layer at 530-650 m has a higher permeability between 205 and 220 md. These values agree well with the core permeability order of 200 md. The permeability values of the two shale layers at 450-530 m and 650-800 m are very small and raging between 65 and 80 μd. The two oil baring sandstone reservoirs have good confining layers according to the permeability images.

CONCLUSIONS

An analytical permeability inversion method and the example permeability images within sandstone oil reservoirs are presented. The velocity and attenuation images measured by the patented PRBS based acoustic crosswell tomography (US Patent No. 5,406,530). The method is shown to be very stable and accurate according to the core permeability results.

ACKNOLEGEMENTS

The analytical permeability inverse of acoustic velocity and attenuation is partly a result of the senior author's research funded by US Office of Naval Research. The PRBS crosswell tomography system was built by YEC for KSC and used during the crosswell tomography experiment by the two authors. All the expenses for the experiment and publication were paid by KSC. TOL provided the two wells for the experiment as well as the down hole logs.

REFERENCES

Yamamoto, T., 1998, A poro-elastic model of extremely permeable limestone for permeability imaging, *Geophysics* (submitted).

Yamamoto, T., Nye, T., and Kuru, M., 1994, Porosity, permeability, shear strength: cross- well tomography below an iron foundry, Geophysics, 59, 1530-1541.

Biot, M. A., 1956, The theory of propagation of elastic waves in a fluid-saturated porous solid, I lower frequency range, J. Accoust. Soc. Am., 12, 155-164.

Mavko, G., and Nur, A., 1975, Melt squirt in asthenosphere, J. Geophys. Res., 80, 1444-1448.

Dvorkin, J., and Nur, A., 1993, Dynamic poroelasticity: a unified model with the squirt and the Biot mechanism, Geophysics, 58, 524-532.

Bregman, N. D., Chapman, C. H., and Baily, R. C., 1989, Travel time and amplitude analysis in values of these sandstone layers, which are of the seismic tomography, J. Geophys. Res., 54, 200-215.

Han, D., Nur, A., and Morgan, D., 1986, Effects of porosity and clay content on wave velocities in sandstones, Geohysics, 51, 2093-2107.

Yamamoto, T., Nye, T., and Kuru, M., 1995, Imaging the permeability structure of a limestone aquifer by crosswell tomography, Geophysics, 60, 1634-1645.

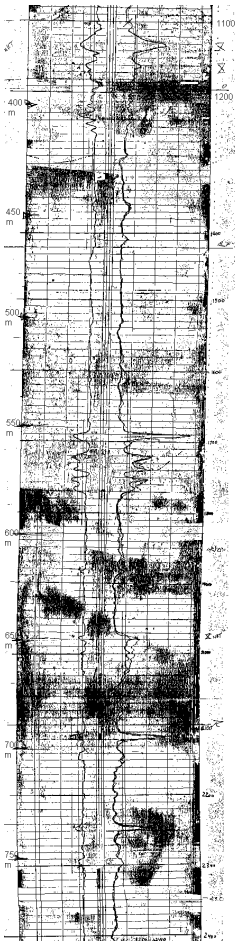

Figure 1a, Resistivity and Gamma Ray Logs, Well Q1.

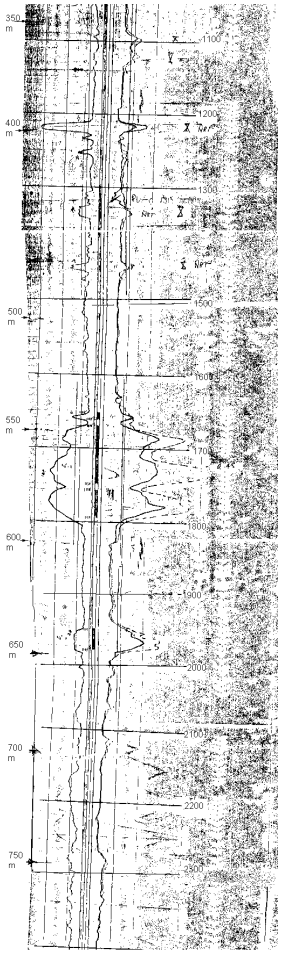

Figure 1b, Resistivity and Gamma Ray Logs, Well MD-15.

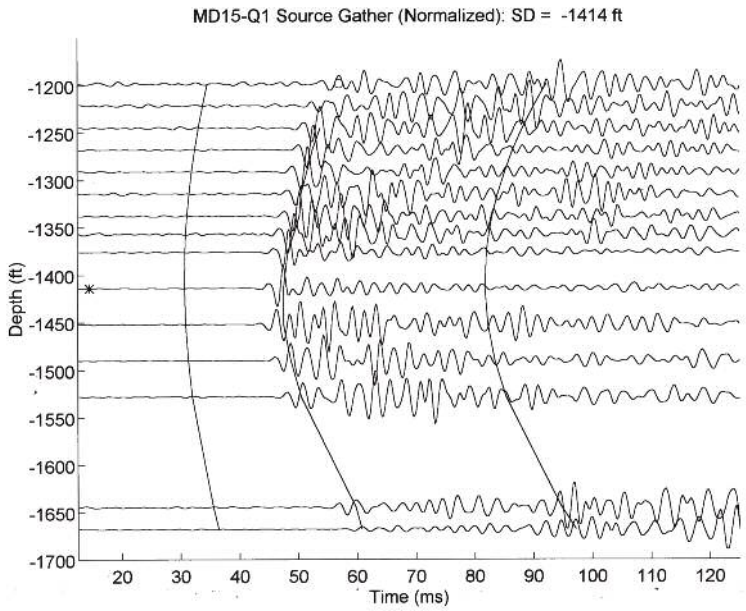

Figure 2, Example 500 Hz PRBS source gather data, source at depth 431(1414 feet) in Well MD15.

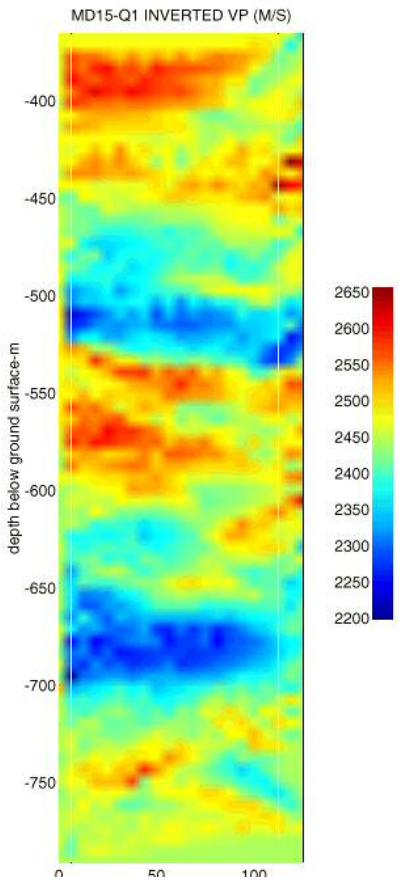

Figure 3a, Velocity image measured at 500 Hz PRBS.

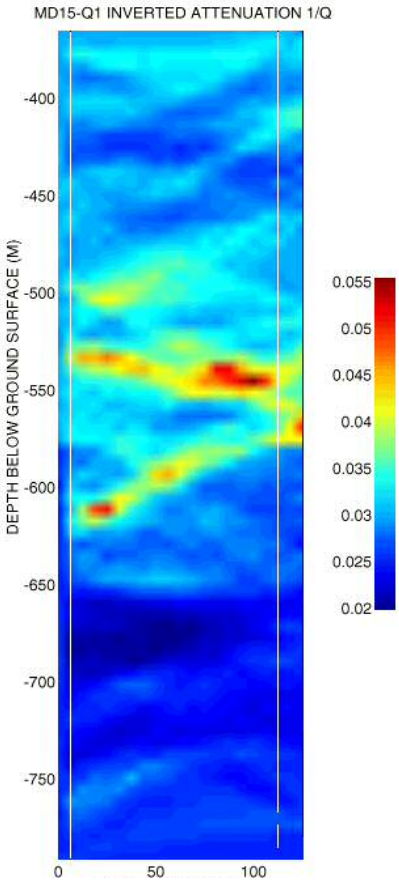

Figure 3b, Attenuation (Q^{-1}) image measured at 500 Hz PRBS.

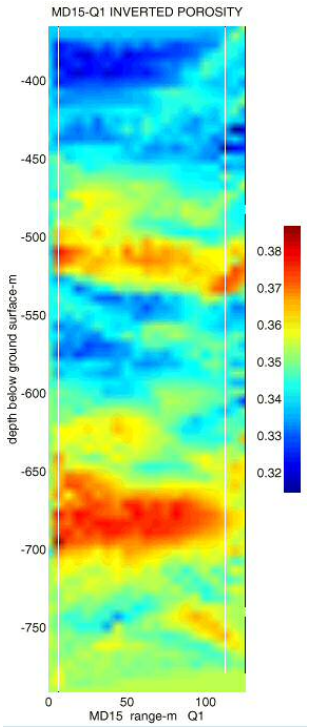

Figure 4a, Porosity image within sandstone layers at 450 to 530 m and 650 to 800 m. Ignore the images in the rest of depth intervals.

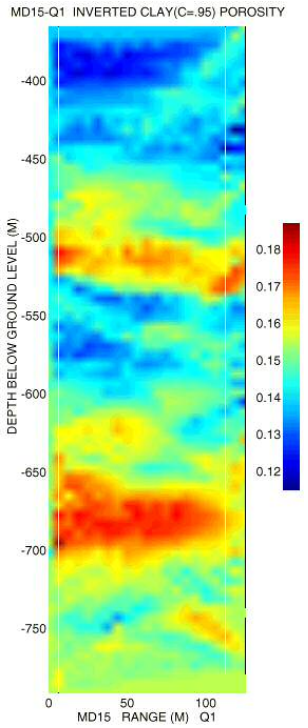

Figure 4b, Porosity image within shale layers at 350 to 450 m and 530 to 650 m. Ignore the images in the rest of depth intervals.

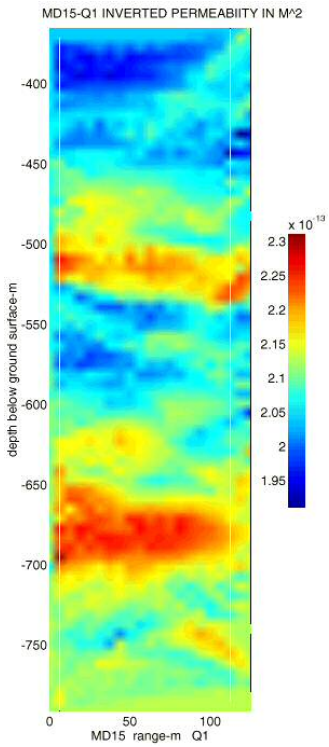

Figure 5a, Permeability image within sandstone layers at 450 to 530 m and 650 to 800 m. Ignore the images in the rest of depth intervals.

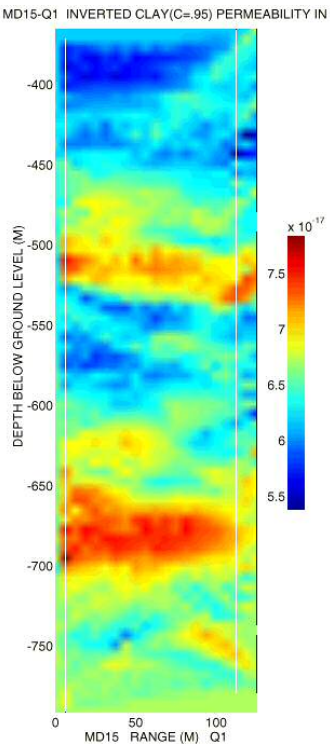

Figure 5b, Permeability image within shale layers at 350 to 450 m and 530 to 650 m. Ignore the images in the rest of depth intervals.